

Wave Run-up and Response Spectrum for Wave Scattering from a Cylinder

Jun Zang

Department of Architecture & Civil Engineering, University of Bath, Bath, UK

Shuxue Liu

The State Key Laboratory of Coastal and Offshore Engineering, Dalian University of Technology, Dalian, PR China

Rodney Eatock Taylor and Paul H Taylor

Department of Engineering Science, University of Oxford, Oxford, UK

ABSTRACT

In this paper, we present both numerical and experimental studies on non-linear wave interaction with a circular cylinder in shallow water and examine the effect of non-linearity on the wave run-up on the structure. Second order wave diffraction theory has been included in the numerical simulation to steep waves. Both the wave run-up time history on the cylinder and the wave response spectrum derived from the diffracted wave time series are investigated and compared with the experiments conducted in a wave tank. Numerical predictions from the second order diffraction simulations agree very well with the experimental measurements for both wave run-up and response spectrum. This validation confirmed that the second order wave diffraction solution works well for steep waves in shallow water, while linear diffraction theory incorrectly predicts the peak water levels and response spectrum.

KEY WORDS: Wave-structure interaction; non-linear wave; circular cylinder; second order wave diffraction; focused waves; shallow water.

INTRODUCTION

Wave diffraction and scattering from coastal and offshore structures are of importance in understanding the impact of non-linear waves on structures, and resulting wave loadings for structural design. Over the past 20 years, research into non-linear wave interaction with deep-water offshore platforms and FPSOs (Kim & Yue (1989, 1990), Chau & Eatock Taylor (1992), Eatock Taylor & Huang (1997), Buldakov et al (2004), Zang et al (2003, 2005, 2006)), has indicated the importance of nonlinear wave theory for estimation and safe offshore design. Second-order wave diffraction theory has been successfully applied to predict non-linear wave forces and free surface elevations around deep water structures.

To achieve the target of 20% of the electricity generated from all sources coming from renewal energy by 2020, it is expected that large numbers of offshore wind turbines will be installed along the UK coast line in the coming decade. Deep water offshore technology,

traditionally used for the development of offshore platforms and floating vessels for the oil and gas industry, is currently used for the development of offshore wind farms. Because the majority of offshore wind turbines are installed in intermediate and shallow waters, where strong non-linear wave interaction with structures cannot be ignored, there is a need to improve our understanding of the effects of wave non-linearity on wave-structure interactions in shallow water.

In this paper, physical experiments and numerical simulations are described for focused waves interacting with a vertical bottom mounted circular cylinder, a typical configuration for an offshore wind turbine foundation. Two test cases with different degrees of non-linearity are examined for both the time history of wave run-up on the structure and the resulting response spectrum. The experiments were conducted in a wave tank in the State Key Laboratory of Coastal and Offshore Engineering, Dalian University of Technology, China. The numerical simulations were produced using DIFFRACT, a second order wave diffraction code, originally written by Chau & Eatock Taylor, and further extended by Zang. Detailed discussions of the effect of non-linearity on wave interaction with such structures in shallow water are given in the paper.

NUMERICAL METHODS

For modelling free surface run-up resulting from non-linear wave interaction with large offshore structures, the assumption of potential flow is reasonable, and the fluid may be taken as incompressible and inviscid, and the flow as irrotational. Then a velocity potential exists which satisfies the Laplace equation

$$\nabla^2\Phi = \frac{\partial^2\Phi}{\partial x^2} + \frac{\partial^2\Phi}{\partial y^2} + \frac{\partial^2\Phi}{\partial z^2} = 0 \quad (1)$$

Two approaches are currently taken for the numerical simulation of non-linear wave interaction with large offshore structures. These are: second order wave diffraction theory and fully non-linear wave diffraction theory. In principle, fully non-linear wave diffraction theory

would account for much higher order components in the solutions, seeming to be the best for simulating strongly non-linear waves and their interaction with bodies, while the second order wave diffraction theory only includes the first and second order terms in a Stokes-type expansion. However in practice, most current non-linear wave simulation methods encounter severe numerical stability problems for the wave-structure interaction problem, and cannot model large near-breaking wave interaction with structures. Such problems are still unsolved, even for regular waves. All these effects limit the applicability of fully non-linear wave models to strongly non-linear wave problems. In contrast to this, second order wave diffraction theory works well and demonstrates its robust ability to provide useful results for the engineering community.

The most important issue involved in the discussion should be the wave interaction with the structure itself. For ship-shaped geometries, our previous study consisting of numerical analysis and physical experiments for a head-on uni-directional steep wave group interaction with a simplified FPSO (Zang, et al 2006), looked for third or higher order harmonic generation from the response spectrum, but if present, these were at a very low level for the ship geometry. This observation also explains why the second order numerical simulation agrees so well with the experiments for the very strong non-linear wave interaction with the FPSO ($ka=0.25$, the largest wave that could be made in the flume without breaking at the ship model).

In this paper, second order wave diffraction theory is employed for the numerical modelling of wave driven flow around the cylinder. The Stokes perturbation method decomposes the velocity potential into terms of different orders. Similarly, the water surface elevation η can also be expressed as a perturbation series. The first order and second order velocity potential must satisfy each of the dynamic and kinematic free surface boundary conditions to that order. The first order and second order free surface boundary conditions at $z=0$ can be expressed as

$$\frac{\partial^2 \Phi^{(1)}}{\partial t^2} + g \frac{\partial \Phi^{(1)}}{\partial z} = 0 \quad (2)$$

$$\begin{aligned} \frac{\partial^2 \Phi^{(2)}}{\partial t^2} + g \frac{\partial \Phi^{(2)}}{\partial z} = & \frac{1}{g} \frac{\partial \Phi^{(1)}}{\partial t} \left[\frac{\partial}{\partial z} \left(\frac{\partial^2 \Phi^{(1)}}{\partial t^2} \right) + g \frac{\partial^2 \Phi^{(1)}}{\partial z^2} \right] \\ & - \frac{\partial}{\partial t} \left[\left(\frac{\partial \Phi^{(1)}}{\partial x} \right)^2 + \left(\frac{\partial \Phi^{(1)}}{\partial y} \right)^2 + \left(\frac{\partial \Phi^{(1)}}{\partial z} \right)^2 \right] \end{aligned} \quad (3)$$

These are necessary, with a no-flow boundary condition on the surface of the structure and at the seabed, together with the far field boundary conditions, in order to construct the complete boundary value problem to second order.

We use here a quadratic boundary element method for the non-linear wave scattering problem. Boundary element methods for first-order diffraction/radiation problems are now widely used in industry. The second-order problem is significantly more difficult to implement due to the non-homogeneous formulation, resulting from the right hand side of Eq. 3, involving the product of linear velocity potentials and their derivatives.

EXPERIMENTAL MEASUREMENTS

As part of the project, physical model tests were performed in a wave tank (69m x 3m) in the State Key Laboratory of Coastal and Offshore

Engineering, Dalian University of Technology (DUT). A single circular cylinder was located in the centre of the tank. A total of 35 wave gauges were arranged around the circular cylinder to examine the wave scattering and wave run-up. The nearest wave gauge to the upstream stagnation point was about 15 mm in front of the cylinder. In order to model a typical offshore wind turbine foundation at laboratory scale, the diameter of the model cylinder used was specified as 0.25 m, and the water depth was 0.5 m. Rather than performing long random wave simulations, we concentrated on focused wave group experiments. NewWave groups (Tromans (1991), Taylor & Vijfvinkel (1998)) with varying wave height and period were used. In the NewWave approach, the focused wave corresponds to the average shape of the largest crest occurring in a random wave series. This captures some of the characteristics of violent wave-structure interactions in an efficient and elegant way. For all focused wave tests, the focus point is fixed at the upstream stagnation point (gauge No.29). The sketch of the experimental model setup is shown in Fig.1.

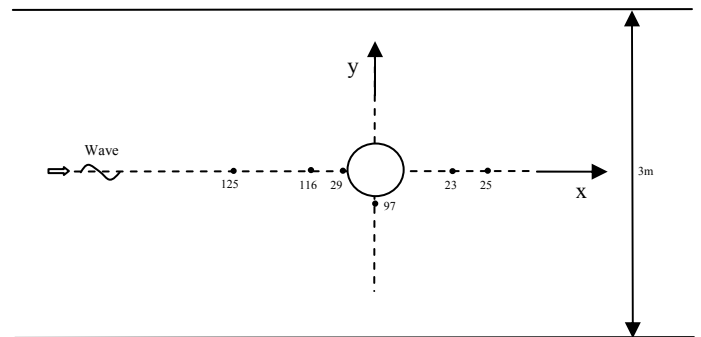


Figure 1 Experimental model setup.

RESULTS AND DISCUSSION

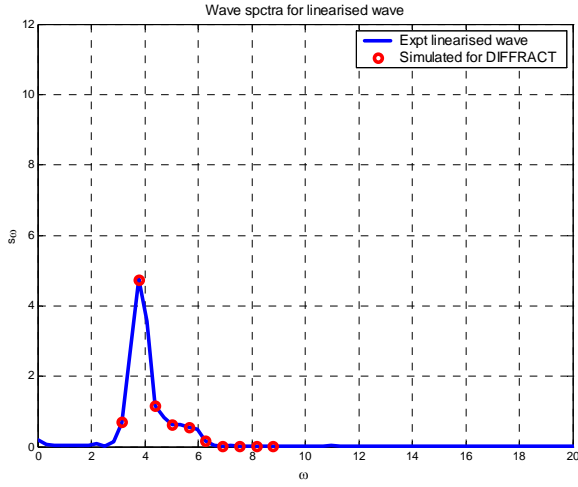
In this section, results from numerical simulations and laboratory measurements are presented for focused wave groups interacting with a vertical bottom mounted circular cylinder. As noted in previous studies on wave diffraction from large offshore structures under uni-directional waves (Buldakov et al (2004), Zang et al (2006)), an approximation to the largest wave run-up on the structure would occur at the front stagnation point. Thus in this paper the main focus is on the front stagnation point. Extensive analysis and discussions on the effect of non-linearity on the wave run-up and response spectrum are given in this section

In order to simulate the experiments, the same incoming wave time history is used for both experiments and numerical calculations. In the NewWave approach, an approximation to the experimental linearized incoming wave time series can be easily obtained from the formula $(C-T)/2$, where C means the measured free surface time history with crest focusing, and T means the measured free surface with trough focusing, both without the cylinder in place. By applying the fast Fourier transform to the experimental linearized incoming wave time series, the corresponding amplitude spectra can be obtained, leading to the results shown in Fig. 2. In this paper, two test cases are considered:

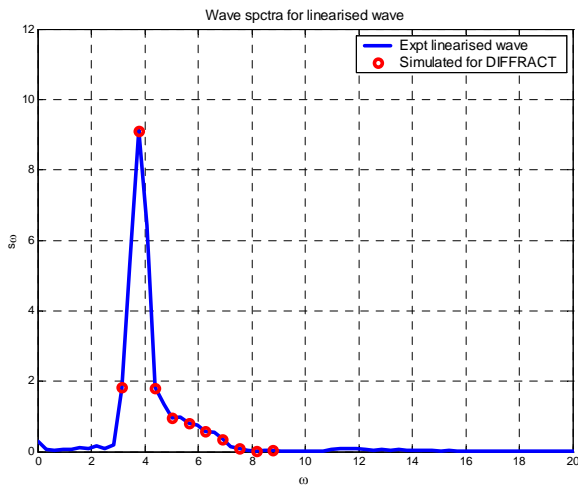
- test case 1: $ka=0.06, kd=0.97$;
- test case 2: $ka=0.12, kd=0.97$,

in which k is defined as the wave number at the peak of the underlying

spectrum, a is the elevation of the wave crest and d is water depth. In both test cases, the wave number and the water depth remain the same: the only difference between the two test cases is the wave steepness, with double the crest elevation being specified in test case 2. For both cases, the NewWave group generated by the paddle was based on a JONSWAP spectrum.



(a)



(b)

Figure 2 Amplitude spectra for linearised incoming wave at the upstream stagnation point. (a) $ka=0.06$, $kd=0.97$. (b) $ka=0.12$, $kd=0.97$.

In order to match the experimental amplitude spectra, 10 chosen frequency components, which are marked by red circles “o” in Fig. 2, have been used in the numerical simulations. If the ocean surface is regarded as a linear random process, the free surface can be represented by

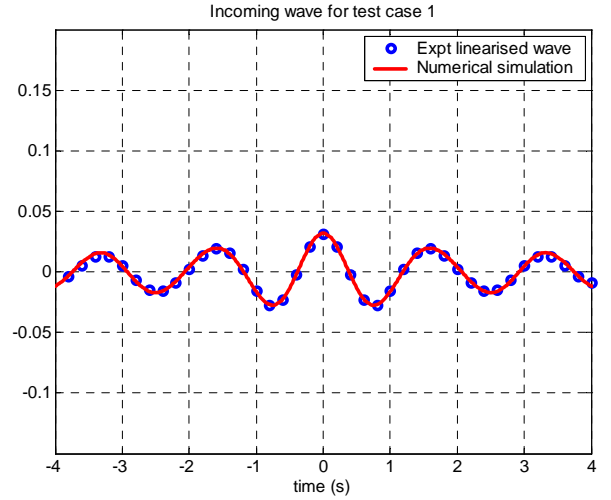
$$\eta = \sum_{j=1}^N A_j \cos(k_j x - \omega_j t + \varepsilon_j) \quad (4)$$

where the amplitude A_j is an appropriate amplitude associated with the frequency component ω_j , and N is the total number of the frequency

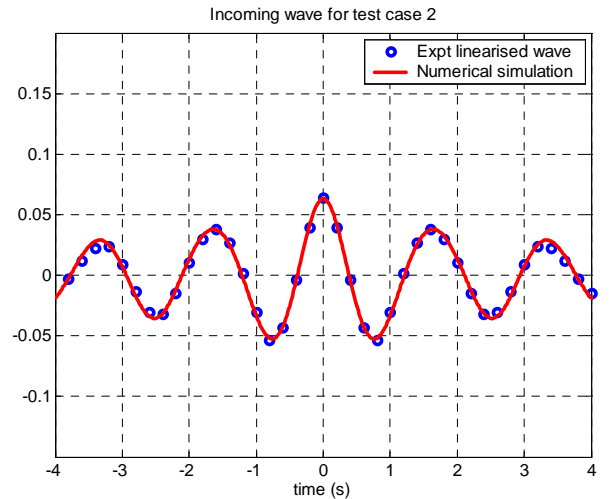
components. If we use the deterministic NewWave concept to model extremes of the surface elevation, it can be written in the form

$$\eta = \alpha \frac{\sum_{j=1}^N S(\omega_j) \Delta \omega \cos(k_j x - \omega_j t + \varepsilon_j)}{\sum_{j=1}^N S(\omega_j) \Delta \omega} \quad (5)$$

where $S(\omega)$ is the wave elevation spectrum, and again α is the amplitude of the extreme elevation. By use of Eq. 5 and the spectra given in Fig.2, the incoming wave time histories can be reproduced. The phase shift ε in eq. (5) is retained to allow for slightly non-perfect focussing.



(a)



(b)

Figure 3 Incoming wave time series at the upstream stagnation point. (a) $ka=0.06$, $kd=0.97$. (b) $ka=0.12$, $kd=0.97$.

Fig. 3 provides a comparison between the numerical simulations of the incident wave group using the 10 chosen frequency components, and the linearized incoming waves, as measured at the upstream stagnation point (Here and in all subsequent plotted time histories of

wave elevation, the units are m). The numerical predictions agree very well with the linearized experimental incoming waves for both test cases. This has provided a solid start for the numerical simulations.

The second order diffraction program *DIFFRACT* based on a quadratic boundary element discretisation was used for the numerical computations. In total, 10 first order diffraction calculations and 55 second order diffraction calculations at pairs of wave frequencies were carried out in the frequency domain (by using symmetry, the results for the remaining pairs in the 10 x 10 matrix can be obtained from the 55 computed pairs). Based on the linear and quadratic transfer functions for free surface elevations at the specified locations in the computational domain, the final diffracted free surface elevations can be constructed to second order using following expressions:

$$\eta(x, t) = \eta^{(1)}(x, t) + \eta^{(2)}(x, t), \quad (6)$$

in which

$$\eta^{(1)}(x, t) = \sum_{j=1}^N A_j (LTF)_j \cos(k_j x - \omega_j t + \varepsilon_j) \quad (7)$$

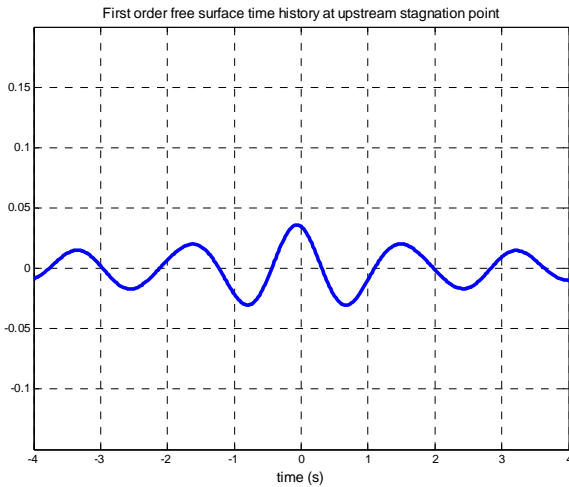
$$\begin{aligned} \eta^{(2)}(x, t) = & \sum_{i=1}^N \sum_{j=1}^N A_i A_j (QTF)_{ij}^s \cos((k_i + k_j)x - (\omega_i + \omega_j)t + \varepsilon_{ij}) \\ & + \sum_{i=1}^N \sum_{j=1}^N A_i A_j (QTF)_{ij}^d \cos((k_i - k_j)x - (\omega_i - \omega_j)t + \varepsilon_{ij}) \\ & + \bar{\eta}^{(2)}. \end{aligned} \quad (8)$$

Here A_i, A_j are the appropriate amplitudes associated with each of the frequency components ω_i, ω_j , in Fig. 2, corresponding to wave numbers k_i, k_j , and $N=10$ is the total number of the frequency components; $(LTF)_i$ is the linear transfer function, $(QTF)_{ij}^s$, and $(QTF)_{ij}^d$ are the quadratic transfer functions for sum and difference frequency components; $\eta^{(1)}$ and $\eta^{(2)}$ are the first order and second order components of the free surface, including both incoming wave and diffracted wave; The term $\bar{\eta}^{(2)}$ is small, being the quadratic time-independent term. In the limit $N \rightarrow \infty$, this term would disappear since it is related to the repeat time of the NewWave based on a Fourier series.

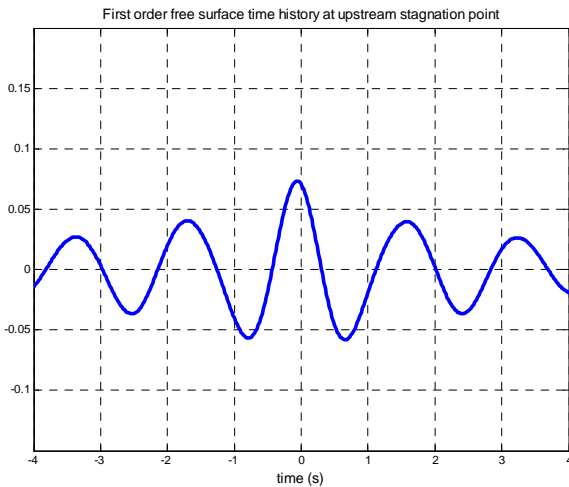
As the focused wave group reaches the cylinder, scattering occurs, resulting in wave diffraction, wave reflection modifying the incoming wave field, and wave run-up on the structure. Fig. 4 presents the computed first order total diffracted wave time history close to the upstream stagnation point. Compared with the incoming wave, the wave enhancement at the front stagnation point due to first order diffraction are 13% and 17% for the two cases, Table 1. It was observed that the first order diffracted wave time histories have roughly the same shape as the incoming wave group. A very small time shift away from the focusing time $t=0$ was found for both wave groups. The difference in the enhancements in the two cases is believed to result from slight differences between the two amplitude spectra in Fig. 2.

By incorporating the second order components of the free surface in the simulation, Fig. 5 compares the total computed 1st plus 2nd order non-linear free surface elevation time histories at the front stagnation point with those measured in the experiments. The red lines present the experimental results, and the blue circles numerical predictions. For both test cases, the numerical predictions match the experimental measurements well, both as to crest values and wave forms.

Compared with the first order diffracted waves shown in Fig. 4, it is obvious that the effect of second order wave diffraction is more significant for the test case 2 with larger wave steepness. The correction from second order wave diffraction not only makes the crest higher, but also changes the wave form significantly for the wave with larger wave steepness. But for waves with weak non-linearity like test case 1, second order wave diffraction is less important. In order to examine the effect of each individual component on the total diffracted free surface, Table 1 lists all the crest values for both test cases, including first order diffracted waves, 2nd order diffracted wave and total 1st plus 2nd order diffracted wave. Note that the incoming wave crest amplitudes a for the two test cases are 0.0315m and 0.063m.



(a)



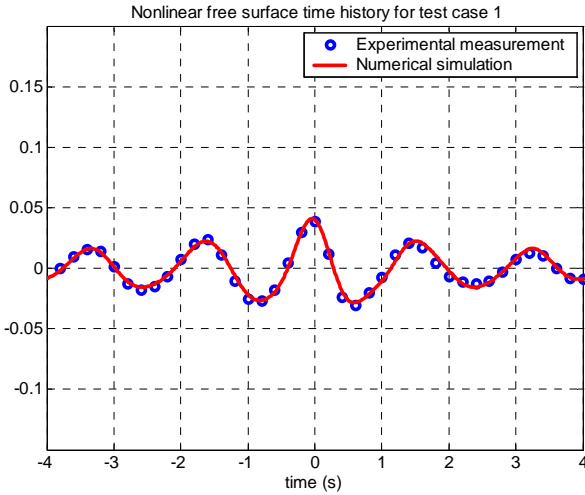
(b)

Fig.4 Computed first order free surface time series at upstream stagnation point.

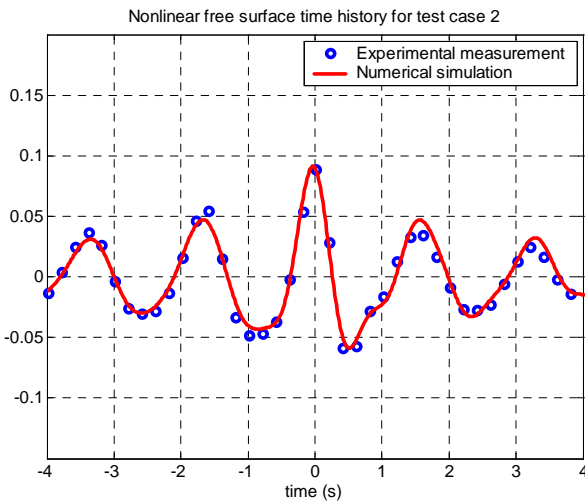
(a) $ka=0.06, kd=0.97$. (b) $ka=0.12, kd=0.97$.

Table 1 1st order, 2nd order and total 1st plus 2nd order free surface at front stagnation point computed using diffraction theory.

	$\eta^{(1)}/a$	$\eta^{(2)}/a$	$(\eta^{(1)} + \eta^{(2)})/a$
Case 1	1.13	0.19	1.32
Case 2	1.17	0.35	1.52



(a)

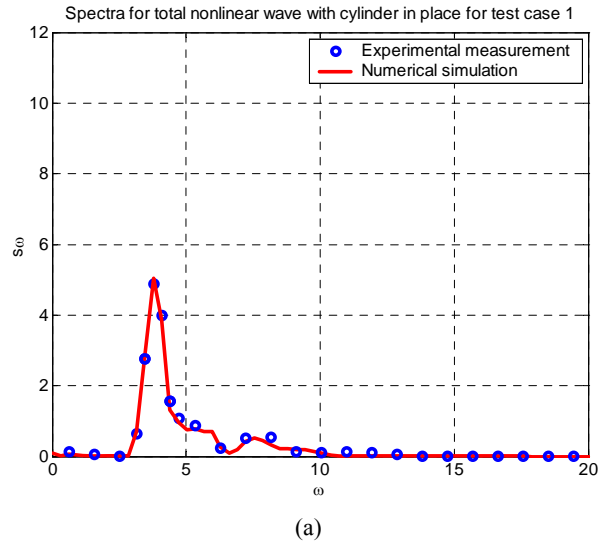


(b)

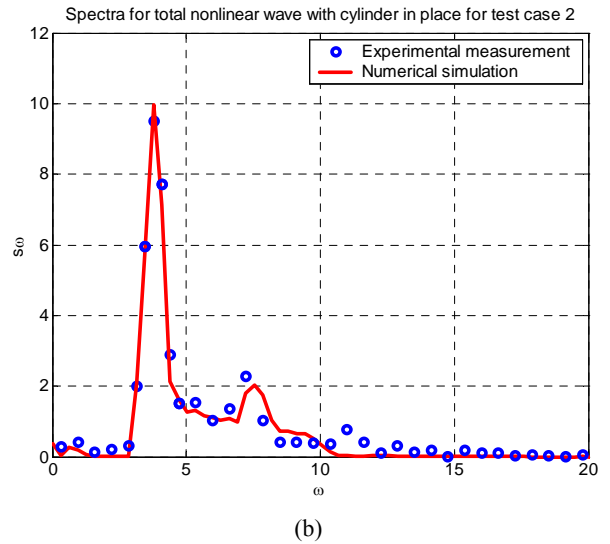
Figure 5 Free surface elevation time histories at the front stagnation point: (a) $ka=0.06, kd=0.97$. (b) $ka=0.12, kd=0.97$.

It is interesting to note how strongly the results of Fig. 5 and the analysis leading to Table 1 support the second order model. The strong second order contribution to the run-up is also seen. Even in the smaller

amplitude wave group, the enhancement due to the second order effect is larger than that resulting from first order diffraction. And this enhancement is then increased by a factor of almost 4 for the larger amplitude group. As a result, in the steep wave case, the upwave run-up is more than 50% higher than the incident wave crest. The radius r of the cylinder (0.125m) corresponds to $kr = 0.24$, suggesting that this is by no means a strongly diffracting structure in these wave groups, at least according to linear theory. The very significant second order contribution, however, suggests otherwise. Ignoring the second order wave diffraction can definitely result in major underestimation.



(a)



(b)

Figure 6 Wave spectra at upstream stagnation point: (a) $ka=0.06, kd=0.97$ (b) $ka=0.12, kd=0.97$.

The amplitude spectra for both numerical results and experimental measurements can be derived from the total diffracted free surface time series via the FFT, as shown in Fig.6. Comparing these with the wave spectra for the linearized incoming waves shown in Fig. 2, we can see that the wave-structure interaction results in not only modest linear enhancement of the free surface around the frequency of the peak, but also strong non-linear contributions beyond the linear frequency range.

For both test cases shown in the paper, second order sum frequency components dominate the total second order contributions. In test case 2 with the steeper incoming wave, a substantial portion of the wave energy is clearly seen in the high frequency zone beyond the linear wave frequency range. The plot of the amplitude spectrum also confirms that the second order numerical simulation correctly predicts the response spectrum for test case 1. This is consistent with the numerical nonlinear diffracted free surface time history matching the experimental result so well. In test case 2, the experimental result plotted in Fig. 6b extends the high frequency tail slightly further than the numerical prediction. This is also reflected in the difference in the wave form in Fig. 5b; though as the energy in the high frequency tail is only a small proportion of the total, the numerical simulation predicts the correct crest value and phase angle, as well as the overall wave form. It would seem likely that the extra energy in the range 10 – 13 rad/s is an indication of some 3rd order contributions to the runup.

Further work is ongoing. The aim is to extend the analysis to points around the circumference of the cylinder, including close to the rear stagnation point. It will be interesting to establish whether 3rd and higher order contributions are larger away from the front stagnation point. Ringing is known to be a design problem for slender columns in deep water. Our experimental analysis aims to see whether similar hydrodynamics is important in shallow water.

The good agreement between the numerical predictions and the experimental measurement for both wave run-up time history and amplitude spectrum suggests that the measured data obtained at DUT are accurate and reliable, and the numerical models are robust and capable of analysing the strong non-linear wave interaction with an offshore wind turbine foundation in shallow water.

CONCLUSIONS

This paper has presented both numerical and experimental studies on non-linear water diffraction by a circular cylinder in shallow water. Two test cases have been carefully chosen and compared to examine the effect of nonlinearity on wave run-up and amplitude spectrum, to improve our understanding of the importance of non-linear wave effects on wave scattering behaviour. The focused wave groups used in both numerical and experimental studies have been proved to be appropriate wave forms to capture the characteristics of violent wave-structure interactions in an efficient and elegant way.

Extensive analysis has been undertaken to compare and interpret the significance of first and second order wave diffraction for waves with different steepnesses in shallow water. On the basis of the two test cases considered in this paper, it has been found that wave enhancement due to second order wave diffraction in shallow water is very significant in the wave field close to the upstream side of the body. For a mild wave with wave steepness $ka=0.1$, the comparison has revealed that the wave enhancement due to the second order wave diffraction is larger than that from the first order wave diffraction. With double the incoming wave amplitude, in test case 2, the wave enhancement due to the second order wave diffraction is seen to be as high as twice that from the first order wave diffraction. From these comparisons it can be concluded that linear diffraction theory incorrectly predicts the magnitude of the peak surface magnifications, while a 2nd-order diffraction solution (i. e. including 1st and 2nd-order components) provides an improved and correct prediction of the extreme water levels and their spectra. Such effects should not be ignored in design.

ACKNOWLEDGEMENTS

The authors gratefully acknowledge financial support from UK EPSRC (Grant No GR/T07220/01 and GR/T07220/2). We are very grateful to Chris Smith, Jinxuan Li and Yan Wang, for their great help with the experiments.

REFERENCES

- Buldakov, EV, Eatock Taylor, R, & Taylor, PH (2004). "Local and far-field surface elevation around a vertical cylinder in unidirectional steep wave groups," *Ocean Engineering*, 31, pp833-864.
- Chau, FP (1989). "The second order velocity potential for diffraction of waves by fixed offshore structures," *Ph.D. dissertation*, University College London, U.K.
- Chau, FP & Eatock Taylor, R (1992). "Second-order wave diffraction by a vertical cylinder," *Journal of Fluid Mechanics*, Vol 240, pp 571–599.
- Eatock Taylor, R & Huang, JB (1997). "Semi-analytical formulation for second-order waves diffracted by a vertical cylinder in bichromatic waves. *Journal of Fluids and Structures*, Vol 11, pp465-484.
- Kim, MH & Yue, DKP (1989). "The complete second - order diffraction solution for an axisymmetric body. Part 1: Monochromatic incident waves," *Journal of Fluid Mechanics*, Vol 200, pp235-264.
- Kim, MH & Yue, DKP (1990). "The complete second - order diffraction solution for an axisymmetric body. Part 2: Bichromatic incident waves and body motions," *Journal of Fluid Mechanics*, Vol 211, pp557-593.
- Taylor PH & Vijfinkel EM (1998). "Focused wave groups on deep and shallow water. *Ocean Wave Kinematics, Dynamics and Loads on Structures, ASCE Proc. of the 1998 International OTRC Symposium*, Houston, pp420-427.
- Tromans, PS, Anaturk, A & Hagemeyer, P (1991). "A new model for the kinematics of large ocean waves – application as a design wave," *Proc. 1st Int. Offshore and Polar Engineering Conference, ISOPE*, Edinburgh, Vol 3, pp64-71.
- Zang, J, Taylor, PH & Eatock Taylor, R (2003). "Hydrodynamics of ship shaped floating platforms," *Report OED/REBASDO/03/04*, University of Oxford.
- Zang, J, Wang, K, Eatock Taylor, R & Taylor, PH (2005). "Second-order wave forces and free surface elevation around a moored ship in steep uni-directional and spread waves." *Proceedings of 4th International Conference on Marine Computational Fluid Dynamics*, Southampton, UK, pp53-38.
- Zang J, Gibson R, Taylor PH, Eatock Taylor R & Swan C (2006). "Second order wave diffraction around a fixed ship-shaped body in unidirectional steep waves," *ASME Journal of Offshore Mechanics and Arctic Engineering*, Vol 128, No 2, pp89-99.